01 Jan 2021

Regional 3D Stability Analyses Of The Egkremnoi Coastline And Comparison With Landslides Caused By The 2015 Lefkada Earthquake

Weibing Gong
Missouri University of Science and Technology, weibing.gong@mst.edu

Dimitrios Zekkos

Marin Clark

John Manousakis

et. al. For a complete list of authors, see https://scholarsmine.mst.edu/geosci_geo_peteng_facwork/2184

Recommended Citation

W. Gong et al., "Regional 3D Stability Analyses Of The Egkremnoi Coastline And Comparison With Landslides Caused By The 2015 Lefkada Earthquake," *Geotechnical Special Publication*, no. GSP 326, pp. 130 - 138, American Society of Civil Engineers, Jan 2021.
The definitive version is available at https://doi.org/10.1061/9780784483435.012

Regional 3D Stability Analyses of the Egkremnoi Coastline and Comparison with Landslides Caused by the 2015 Lefkada Earthquake

Weibing Gong, S.M.ASCE[1]; Dimitrios Zekkos, Ph.D., P.E., M.ASCE[2]; Marin Clark, Ph.D.[3]; John Manousakis[4]; and Dalia Kirshbaum, Ph.D.[5]

[1]Dept. of Civil and Environmental Engineering, Univ. of California, Berkeley, CA. Email: wbgong@berkeley.edu
[2]Dept. of Civil and Environmental Engineering, Univ. of California, Berkeley, CA. Email: zekkos@berkeley.edu
[3]Dept. of Earth and Environmental Sciences, Univ. of Michigan, Ann Arbor, MI. Email: marinkc@umich.edu
[4]Elxis Group, Athens, Greece. Email: jmanousakis@elxisgroup.com
[5]NASA Goddard Space Flight Center, Greenbelt, MD. Email: dalia.b.kirschbaum@nasa.gov

ABSTRACT

Regional three-dimensional (3D) forward modeling stability analyses are presented for the Egkremnoi coastline of Lefkada Island in Greece. The pre-earthquake 5-m resolution DEM of the region was used as input for the regional 3D model and the modeling results were evaluated for five large landslides that occurred in the area during a M_w 6.5 earthquake that occurred in 2015. The area ratio and the overlap area ratio were defined to quantitatively assess the geospatial "match" between predicted and mapped landslides. Parametric analyses using variable material strength and DEM resolution were subsequently conducted to assess the influence of the input on the estimates of factor of safety, geometry, and location for the predicted most critical landslide. For the cases studied here, the assumed material strength has a greater influence on the factor of safety compared with DEM resolution. However, we find that the DEM resolution has a more pronounced influence on the location and size of predicted landslides.

INTRODUCTION

The ability to perform stability analyses over large areas has the potential to lead to better assessments of landslide susceptibility and improved risk assessment. As such, understanding the influence of input parameters on the results of regional 3D stability analyses is an open avenue of research because higher quality spatial datasets have become available and computational frameworks have become inexpensive and easier to use. Specifically, the influence of topography resolution and assumed material strength on the results of regional 3D simulation results needs to be better understood. In this paper, we utilize forward-modeling, predictive, 3D limit equilibrium analyses of the Egkremnoi coastline and compare the results to mapped landslides that occurred during the M_w 6.5 November 17 2015 earthquake event. This earthquake event caused nearly 700 co-seismic landslides along the western coastline of the island. The co-seismic landslides were mapped in three dimensions using satellite and UAV-based 3D models and imagery (Zekkos et al. 2017; Zekkos et al. 2018; Zekkos and Clark 2020). Recently, Kallimogiannis et al. (2019) conducted a 3D back-analysis of one landslide in this area and found strength parameters that best match the landslide geometry. Additional rock mass characterizations have been done by Grendas et al. (2018) and Valkaniotis et al. (2018). In this study, we perform stability analyses using a range of input parameters along sections where the five largest co-seismic landslides occurred, without forcing the predicted failure surface to match the mapped landslide. The resemblance of the predicted landslide geometries and locations to the mapped landslides is then considered. For the five landslides being considered (Landslide 1 to Landslide 5 in Figure 1), the mapped plan-view areas are 13390 m^2, 4998 m^2, 6633 m^2, 8586 m^2 and 7815 m^2, respectively.

Figure 1. Selected mapped landslides in Egkremnoi region

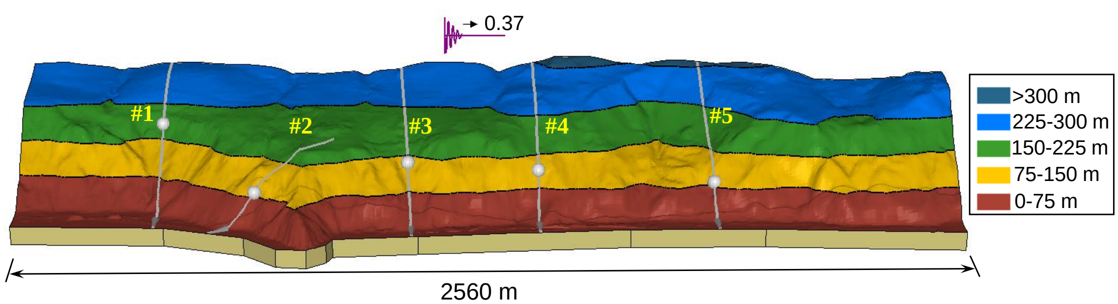

Figure 2. Regional 3D model with analysis planes corresponding to centroids of mapped landslides numbered 1 through 5

PROCEDURES FOR BUILDING REGIONAL 3D MODEL

A 5-m pre-earthquake DEM generated in 2009 for the Hellenic Cadastre was used as input in the analysis. Five analysis planes were selected so that they intersect the centroid of each of the five mapped landslides, but the planes extend to the ends of the model in both the uphill and downhill direction (except for Landslide 2) for an approximate length of 600 m. One million trial failure searches were analyzed for each analysis plane. The Spencer's limit equilibrium method (Spencer 1967; SoilVision System 2019) was adopted to estimate the 3D stability of trial failure surfaces. Because the DEM resolution was 5 m, the regional 3D model was divided into 5 m × 5 m columns. The material strength is described by the Mohr-Coulomb criterion, and no water table was considered in the analyses because the coastal slopes were generally dry at the time of the earthquake. The seismic force was simplified as a constant horizontal force equal to the product of the weight of potential failure mass and the pseudo-static coefficient and was applied though the centroid of failure mass with a vector direction parallel to the sliding direction. Based on the available in-situ shear wave velocity measurements and the estimated stiffness of the landslides, the site periods of the landslides were found to be 0.04 sec and thus the pseudo-static coefficient was set equal to the peak ground acceleration (PGA), which is 0.37g (ShakeMap, U.S. Geological Survey 2015). The 3D model used in the analyses is shown in Figure 2. The analyses were conducted using the software SoilVision (Bentley Systems 2020).

RESULTS AND DISCUSSIONS

Forward Modeling Results

In this study, since the landslides occurred within the same geologic unit, a uniform material strength was assumed for fractured to disintegrated limestone rocks (Ganas et al. 2016; Zekkos and Clark 2020). The cohesion, c, and the friction angle, φ were varied by 1 kPa and 1°, starting with a baseline estimate of $c = 30$ kPa and $\varphi = 30°$, which were considered low for the limestones encountered in this area. It was found that for cohesion equal to 40 kPa and friction angle equal to 48°, the predicted landslides were similar to the mapped landslides, and the factors of safety of Landslides 1-3 and 5 were equal to 1 while the factor of safety of Landslide 4 was 0.85. Higher strength parameters resulted in pseudo-static factors of safety greater than 1 for some of the landslides, or greater differences in the size and location of the modelled landslides compared to the mapped. A comparison of the predicted and mapped landslides for the "best-match" strength parameters is shown in Figure 3. All the predicted landslides have some overlap with the mapped landslides.

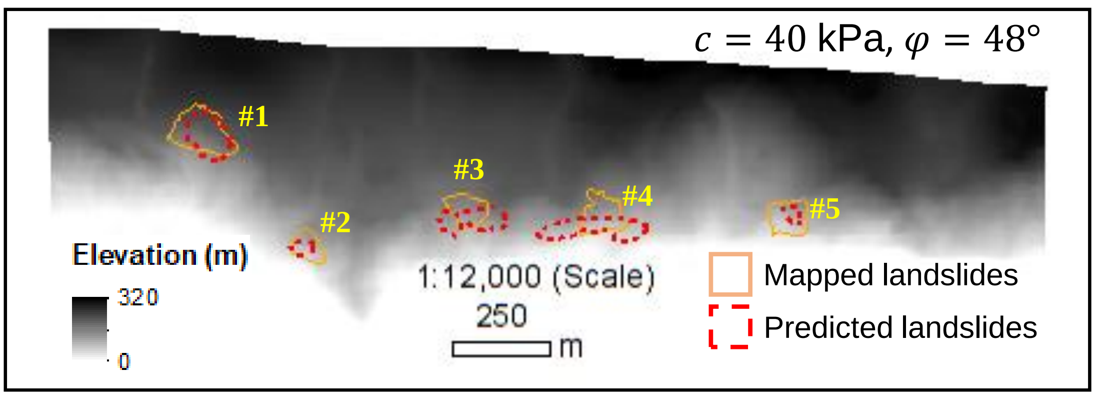

Figure 3. Comparison between mapped and predicted landslides

To quantify the comparison between mapped and predicted landslides, two parameters, the area ratio, R_A, and the overlap area ratio, R_{OA}, were defined as follows:

$$R_A = \frac{A_P}{A_M} \quad (1)$$

$$R_{OA} = \frac{A_O}{A_M} \quad (2)$$

where A_M is the area of mapped landslide; A_P is the area of its predicted counterpart; and A_O is the overlap area. In the case of a perfect match between a predicted landslide and a mapped landslide, R_A and R_{OA} should both be equal to 1.

Figure 4 illustrates the results of the analyses for the five predicted landslides using the R_A and R_{OA} parameters. Predicted Landslide 1 matches the mapped landslide well, as the entire predicted landslide nearly overlaps the mapped and their sizes are similar. Predicted Landslides 3 and 4 are also reasonably consistent with their mapped counterparts. Predicted landslides 2 and 5 both underestimate the mapped area and have a small amount of overlap with the mapped landslides. It is important to note that for this forward modeling predictive analysis, the goal is not to back-calculate each individual landslide, but to find a regional strength estimate that best matches the observed landslides for the entire area (i.e., all landslides). As a result, even for the "best-match" strength parameters the ratios are not very close to one. Varying the strength parameters for each of the mapped landslides, as done by Kallimogiannis et al. (2019), is appropriate for back-analysis and will provide a better match between modeled and mapped landslides, but this process is time-consuming and possible only as a back-calculation (i.e., when landslides have already occurred).

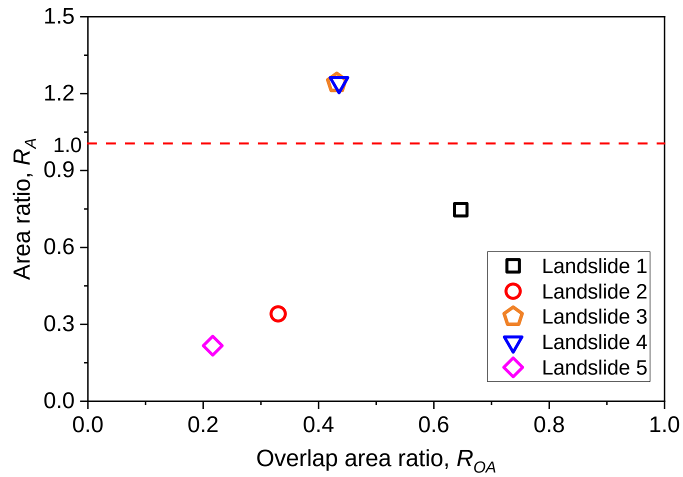

Figure 4. Calculated area ratio R_A, and overlap area ratio R_{OA} for the five landslides considered in this study.

Parametric Analyses

Parametric analyses were also performed to assess the influence of input parameters on the results. First, the influence of cohesion and friction angle on the results is assessed. Subsequently, the influence of topography resolution on the results is investigated. Understanding the influence of the DEM resolution is important because although with advances in technology high-resolution DEMs are more likely to become available, for the majority of the planet, the available DEM may be as coarse as 30 m horizontal resolution.

Effects of material properties on predicted landslides

Figure 5 shows a comparison of predicted landslides for a constant friction angle of 40° and varying cohesion. For Landslides 1 and 2, the predicted landslides overlap with the mapped landslides and are generally located in the same critical area along the plane. However, the location of the critical landslides for Landslides 3-5 have greater variance depending on the cohesion. Figure 6 summarizes the results in terms of calculated factor of safety, area, volume, and average depth of predicted landslides. The area, volume and landslide average depth results in Figure 6b-d are normalized against the results for $c = 30$ kPa and $\varphi = 40°$. As expected and shown in Figure 6a, the factors of safety increase with an increase in cohesion for all analysis planes. However, the increase in factor of safety is not the same for all landslides. For example, for the sections going through Landslides 4 and 5, the factors of safety increase about 50% as the cohesion increases from 40 kPa to 100 kPa, while for the other three sections the increase in factor of safety is significantly lower than 50%. The volume and area of the predicted landslide generally increase as cohesion increases. However, for Landslides 3 and 4 and when $c = 100$ kPa, the location of the predicted landslides changes to a greater degree and the landslides are smaller in size.

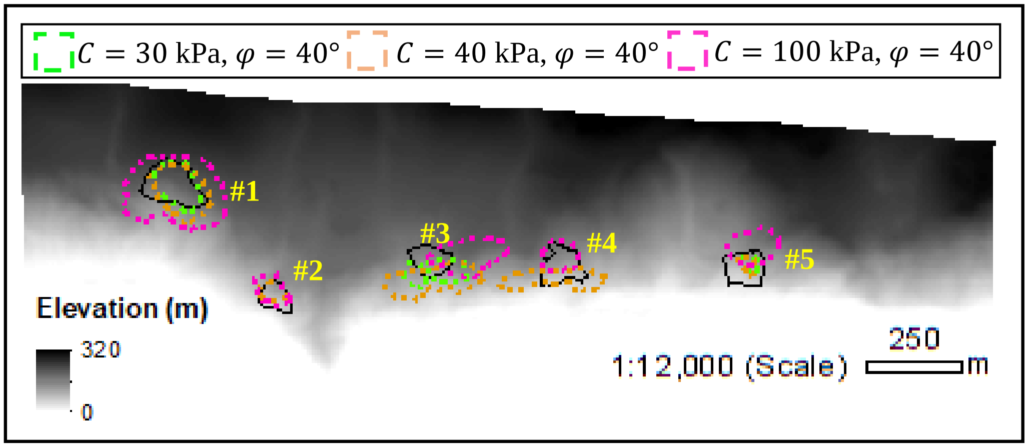

Figure 5. Comparison of mapped landslides (solid black lines) and predicted landslides for different cohesions (dashed lines)

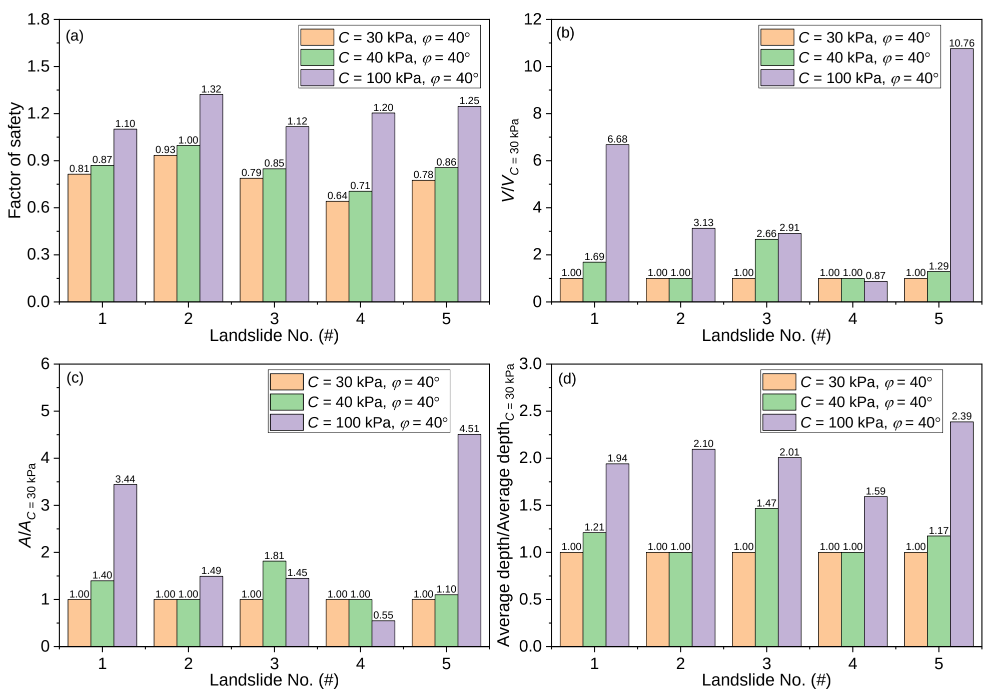

Figure 6. Calculation of results with different cohesions depending on (a) factor of safety; (b) volume; (c) area; and (d) average depth. Volume, area and average depth results are normalized against results for $c = 30$ kPa and $\varphi = 40°$.

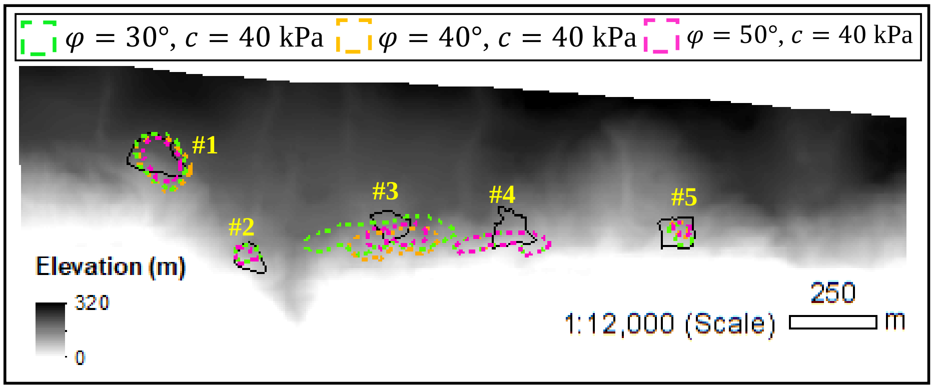

Figure 7. Comparison of mapped landslides (black solid lines) and predicted landslides with different friction angles (dashed lines)

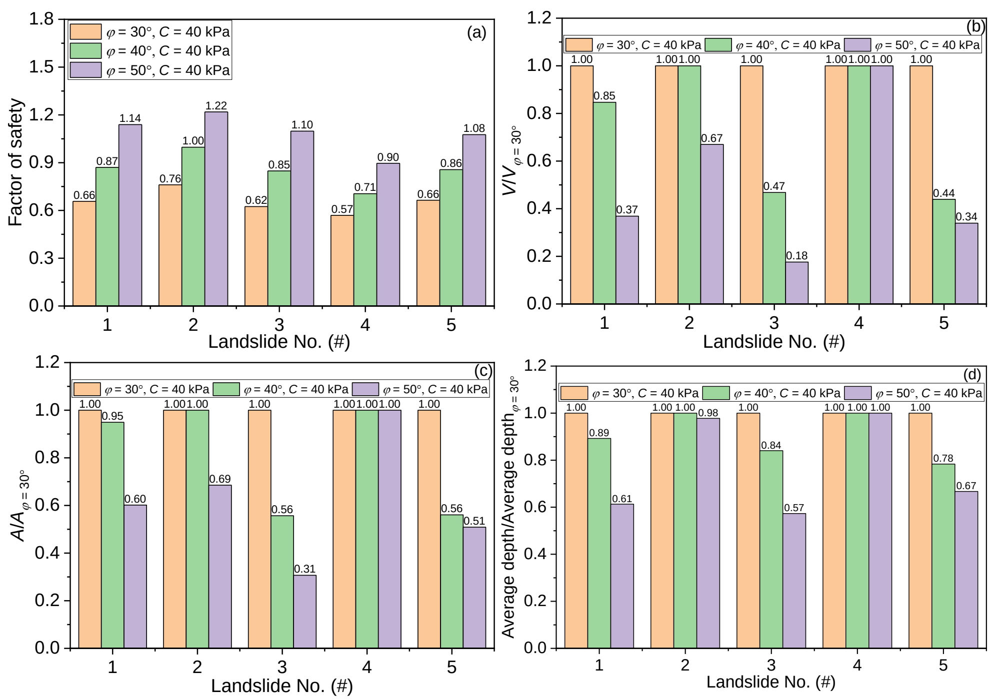

Figure 8. Calculation of results for different friction angles depending on (a) factor of safety; (b) volume; (c) area; and (d) average depth. Volume, area and average depth results are normalized against results for $c = 30$ kPa and $\varphi = 40°$.

The location and geometry of predicted landslides with $c = 40$ kPa and varying friction angles is shown in Figure 7. In general, the size of predicted landslides decreases with an increase in friction angle, however the size of predicted Landslide 4 remains practically the same for all the friction angles considered. The location of all predicted landslides is similar for friction angle ranges from 30° to 50°. The factor of safety and the sizes of predicted landslides for different friction angles are summarized in Figure 8. The results in Figures 8b-c are normalized against the results for $\varphi = 30°$ and $c = 40$ kPa. Figure 8a shows that the factor of safety increases similarly with an increase in friction angle for all analysis planes. The volumes, areas and average depths of predicted landslides in Figures 8b-c decrease as the friction angle increases. This is most obvious for Landslides 1 and 2 where for a friction angle increase from 40° to 50°, volumes and areas decrease by about 50%. For Landslides 3 and 5, the decreasing trends of volume, area and average depth are greater for friction angle increases between 30° and 40°.

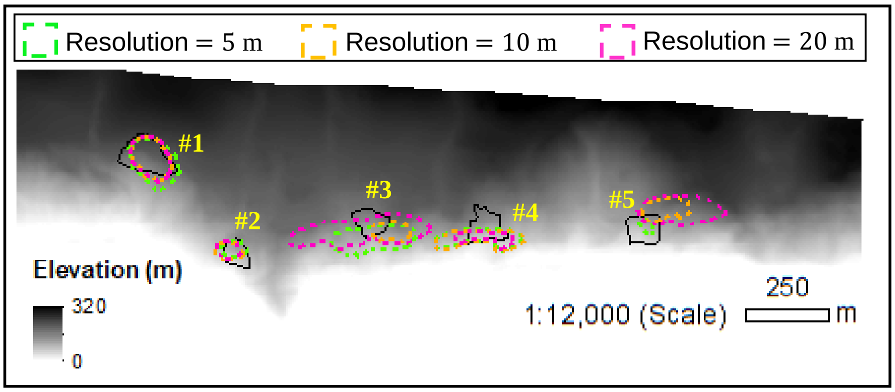

Figure 9. Comparison of mapped landslides (black solid lines) and predicted landslides with different DEM resolutions (dashed lines)

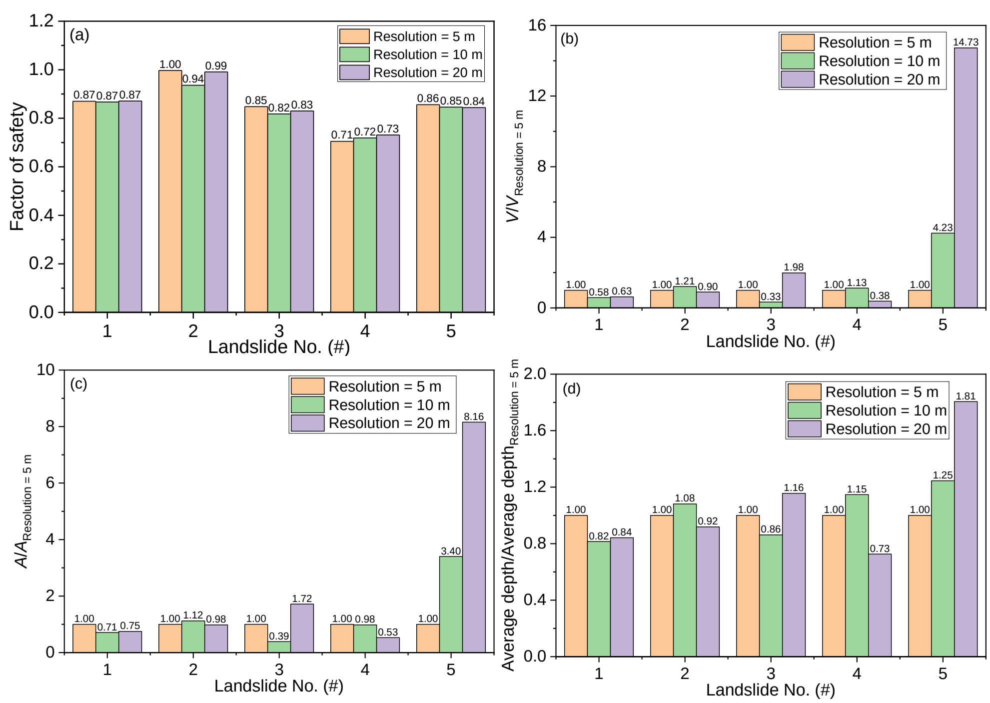

Figure 10. Calculation of results with different DEM resolutions depending on (a) factor of safety; (b) volume; (c) area; and (d) average depth. Volume, area and average depth results are normalized against results for 5-m DEM.

Effects of DEM resolution on predicted landslides

To investigate the effect of DEM resolution on the geometry and location of landslides, 3D stability analyses were performed on the 5-m resolution DEM, as well as downgraded resolutions of 10-m and 20-m (Figure 9). Landslides 1 and 2 have similar sizes and locations regardless of DEM resolution. The sizes of Landslides 3 and 4 change with the DEM resolution, but not systematically. The size of predicted Landslide 5 increases with a decrease in resolution and the volume of 20-m resolution model is about 3.5 times larger than the volume of the landslide using the 10-m resolution model and 14.7 times larger than that for the 5-m resolution model (Figure 10). Additionally, the location of predicted Landslide 5 changes more significantly than the other landslides with very little overlap with the mapped landslide (Figure 9). For the considered analysis planes, the factors of safety are nearly identical for different DEMs. Therefore, for these landslides, although DEM resolution affects the sizes and location of predicted landslides, it has a small influence in the calculated factor of safety.

CONCLUSIONS

Regional 3D forward modeling stability analyses were conducted in the Egkremnoi area of the western coastline of Lefkada, targeting five mapped landslides that occurred during the 2015 Lefkada earthquake and had plan-view areas that ranged between 5000 and 13390 m^2. The area ratio and the overlap area ratio were used to assess the “best-match” between predicted and mapped landslides. The effects of DEM resolution and material properties on predicted landslides were investigated. The results show that the factor of safety is significantly affected by the variations in the cohesion and friction angle but not sensitive to the decrease in DEM resolution. The location of predicted landslides can change due to the variations in cohesion and DEM resolution, but this does not seem to occur for variation in friction angle (from 30°-50°). The size of predicted landslides increases with an increase in cohesion unless the location of predicted landslides changes significantly, while an increase in friction angle results in a decrease in the size of landslides. The decrease in DEM resolution influences the size of predicted landslides, but not systematically.

ACKNOWLEDGEMENTS

This study is financially supported by USGS National Earthquake Hazards Reduction Program (NEHRP) under Grant No. G17AP00088 and by NASA under Grant No. 18-DISASTER18-0022.

REFERENCES

Bentley Systems. (2020). *SOILVISION Edition V10*. Exton, Pennsylvania, United States.

Ganas, A., Elias, P., Bozionelos, G., Papathanassiou, G., Avallone, A., Papastergios, A., Valkaniotis, S., Parcharidis, I., and Briole, P. (2016). Coseismic deformation, field observations and seismic fault of the 17 November 2015 M= 6.5, Lefkada Island, Greece earthquake. *Tectonophysics*, 687, 210-222.

Grendas, N., Marinos, V., Papathanassiou, G., Ganas, A., and Valkaniotis, S. (2018). Engineering geological mapping of earthquake-induced landslides in South Lefkada Island, Greece: evaluation of the type and characteristics of the slope failures. *Environmental Earth Sciences*, *77*(12), 425.

Kallimogiannis, V., Saroglou, C., Zekkos, D., and Manousakis, J. (2019) 2D and 3D Back-analysis of a landslide in Egremnoi caused by the November 17 2015 Lefkada earthquake. In *2nd International Conference on Natural Hazards & Infrastructure*, Chania, Greece.

Spencer, E. (1967). A method of analysis of the stability of embankments assuming parallel inter-slice forces. *Géotechnique*, 17(1), 11-26.

SoilVision Systems Ltd. (2019). *SVSLOPE Theory Manual*. Saskatoon, Saskatchewan, Canada.

U.S. Geological Survey. (2015). Advanced National Seismic System (ANSS), ShakeMap, Global Region, Maps of ground shaking and intensity for event us10003ywp, GREECE. https://earthquake.usgs.gov/earthquakes/eventpage/us10003ywp/shakemap/pga?source=us&code=us10003ywp.

Valkaniotis, S., Papathanassiou, G., and Ganas, A. (2018). Mapping an earthquake-induced landslide based on UAV imagery; case study of the 2015 Okeanos landslide, Lefkada, Greece. *Engineering geology*, *245*, 141-152.

Zekkos, D., and Clark, M. (2020). Characterization of landslides and rock mass strength leveraging the 2015 Mw 6.5 Lefkada Earthquake in Greece. Final Technical Report. U.S. Geology Survey. National Earthquake Hazards Reduction Program, Award Number G17AP00088.

Zekkos, D., Clark, M., Cowell, K., Medwedeff, W., Manousakis, J., Saroglou, H., and Tsiambaos, G. Satellite and UAV-enabled mapping of landslides caused by the November 17th 2015 Mw 6.5 Lefkada earthquake, in: *Proc. 19th Int. Conference on Soil Mechanics and Geotechnical Engineering*, 17–22 September 2017, Seoul, 2017.

Zekkos, D., Greenwood, W., Lynch, J., Manousakis, J., Athanasopoulos-Zekkos, A., Clark, M., and Saroglou, C. (2018). Lessons learned from the application of UAV-enabled structure-from-motion photogrammetry in geotechnical engineering. *International Journal of Geoengineering Case Histories*, 4, 254-274.